

# Compression creep of molten poly(ethylene oxide)

J. V. Aleman

*Instituto de Ciencia y Tecnología de Polímeros, Juan de la Cierva C, 28006 Madrid, Spain*

*(Received 24 May 1990; revised 31 July 1990; accepted 31 July 1990)*

Viscoelastic parameters of poly(ethylene oxide) in compression creep have been measured. Volume deformations ( $k\%$ ) increase as pressure ( $P$ ) and temperature ( $T$ ) increase. Bulk creep compliance  $B(t)$  behaviour is different below and above certain critical values ( $T_c \approx 393$  K, and  $P_c \approx 30$  MPa) assumed to correspond to the transition from helicoidal to planar conformations. Plots of  $B(t)$  versus time ( $t$ ) may be shifted to provide master curves, the pressure shift factors ( $b_p, a_p$ ) and the temperature shift factors ( $b_T, a_T$ ) increasing non-linearly as the pressure and temperature increase. The steady-state creep compliance ( $B^s$ ) allows determination of the recoverable elastic energy ( $B_e$ ). Volume viscosity ( $\eta_K$ ) above 30 MPa remains almost constant, but decreases with increasing temperature.

(Keywords: poly(ethylene oxide); creep; viscoelasticity)

## INTRODUCTION

Polymer bulk compression creep has received little attention to date<sup>1,2</sup> due to the inherent practical difficulties related to precise measurement of volume deformations, and the commonly accepted notion that almost no significant volume change takes place in practice.

A need is felt for compression creep data because of the practical relevance of the transient response of materials. Instantaneous (equilibrium) behaviour of solid polymers in compression has received some consideration<sup>3</sup>. The delayed behaviour has been measured dynamically since the deformation applied is small and therefore the free volume non-linear behaviour does not greatly affect the results<sup>3</sup>.

The time-dependent volume changes (compression creep) of molten polymers have been described to date for rigid polymers (see Appendix A), such as poly(butylene terephthalate) (PBT)<sup>1</sup> (planar chains with aromatic rings, and  $-\Delta F^{600K} = 458$  J g<sup>-1</sup>), and polystyrene (PS)<sup>2</sup> (helicoidal chains with side-groups and  $-\Delta F^{450K} = 500$  J g<sup>-1</sup>).

In order to further explain the effect of chain structure on the creep behaviour, polymers with flexible chains (see Appendix A) ( $-\Delta F^{450K} \approx 200$ – $250$  J g<sup>-1</sup>) and long branches (low density polyethylene (LDPE) planar, non-polar)<sup>4</sup>, as well as linear chains (poly(ethylene oxide) (PEO), helicoidal, polar)<sup>5</sup> are being studied. This paper deals with the compression creep behaviour of molten PEO.

## EXPERIMENTAL

### Materials

Polyox WSRN 750 was provided by the Union Carbide Corporation (Belgium). Its molecular characteristics have been described elsewhere<sup>5</sup>.

A silicone lubricant type Rhodosil 47-V-300 from

Siliconas Hispanicas SA (Spain) was used to avoid friction at the walls.

### Method

All compression measurements were carried out in an Instron Capillary Rheometer attached to an Instron Tensile Tester model TT-CM, with a steel plug instead of the capillary, as described in Figure 1 of ref. 6.

The rheometer barrel (area  $A = 0.907$  cm<sup>2</sup>) was preheated to 303 K. Dial reading provided the zero setting ( $l^0$ ). Then 4.5 g PEO in the form of powder were added, and a Rulon plug, length  $l_r$ , was introduced into the cylinder. A vacuum of 0.2 mmHg was applied for 30 min while raising the temperature to 328 K for the absorbed water to evolve. (At 75% r.h. the PEO absorbs 3–5% by weight of surface water<sup>7</sup> which is easily removable.) The barrel was then heated to the run temperatures of 373–412 K (degradation of PEO occurs at temperatures above 423 K)<sup>7,8</sup>. The equilibrium in force ( $F$ ) and temperature ( $T$ ) was attained under a load of 1 kg. Since the experimental temperatures were well above the polymer melting temperature ( $T_m = 349$  K) the thermodynamic equilibrium was rapidly established. The initial volume of polymer ( $V_0$ ) is consequently a function of temperature only.

Machine cross-head was lowered at selected rates (usually 2 cm min<sup>-1</sup> for the 5 MPa and 30 MPa runs, 5 cm min<sup>-1</sup> for the 70 MPa and 100 MPa runs and 10 cm min<sup>-1</sup> for 130 MPa and 170 MPa runs) in order to achieve the pressure ( $P = F/A$ ) chosen for the experiment (5–170 MPa). Pressure was then kept constant while the changes in length ( $\Delta l_c$ ) with time ( $t$ ) were recorded. Actual results are shown in Figure 1 at 373 K and 70 MPa as a representative example.

The initial length ( $l_i$ ) was computed from the cross-head speed, the Instron paper speed (20 cm min<sup>-1</sup>) and the paper length ( $l_p$ , cm) between the point at which the force started to increase and that at which it reached

the constant value selected (at which the dial reading after 10 s was  $l_{10^0}$ ):

$$l_i = 0.25 \times l_p + l_{10^0} \quad (1)$$

The actual initial length of polymer ( $l_0$ ) is:

$$l_0 = l_i + l_s - l_r \quad (2)$$

in which  $l_s$  (1.25 cm) is the plunger travel security length. Thus it was possible to calculate the initial volume of polymer:

$$V_0 = V_{0.1,T,0} = \pi R^2(l_0 - l^0) \quad (3)$$

The length of polymer at any time ( $l_t$ ) was then computed:

$$l_t = \Delta l_c + l_s - l_r + (\Delta l_r + \Delta l_{app})_c \quad (4)$$

in which  $\Delta l_r$  is the change with pressure of the Rulon plug length, and  $\Delta l_{app}$  is the compliance (background response) of the experimental equipment<sup>2</sup>. The volume  $V_c$  at  $t = t_c$  is therefore:

$$V_c = V_{P,T,t} = \pi R^2(l_t - l^0) \quad (5)$$

Dial reading was continued until the steady state volume was attained. Polymer decompression was then started by reducing the pressure of the system to a constant value of 1 or 2 MPa, according to the run being carried out. The increase in polymer length ( $\Delta l_d$ ) with time was registered.

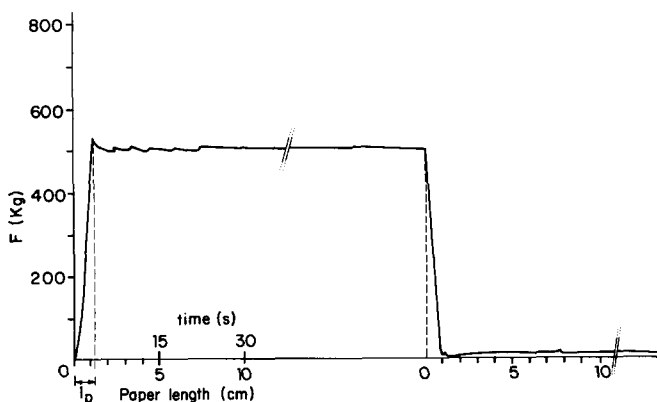


Figure 1 PEO force ( $F$ ) versus time (paper length  $l_p$ ) at 373 K and 70 MPa

The length of polymer ( $l_d$ ) at  $t = t_d$  is now:

$$l_d = \Delta l_d + l_s - l_r + (\Delta l_r + \Delta l_{app})_d \quad (6)$$

The decompression volume is:

$$V_d = \pi R^2(l_d - l^0) \quad (7)$$

The change in volume of the sample:

$$\Delta V_c = V_0 - V_c \quad (8)$$

$$\Delta V_d = V_0 - V_d \quad (9)$$

The experimental procedure was tested with poly(ethylene terephthalate)<sup>1,9</sup>.

## RESULTS AND DISCUSSION

$\Delta V$  values at temperatures 373, 383, 393, 403 and 412 K, and pressures 5, 30, 70, 100, 130 and 170 MPa, were used to compute the volume deformations ( $k\%$ ):

$$k_c\% = \frac{\Delta V_c}{V_0} \times 100 \quad (10)$$

$$k_d\% = \frac{\Delta V_d}{V_0} \times 100 \quad (11)$$

These values are plotted versus time ( $t$ ) in Figures 2a and 2b at 403 K and 30 MPa respectively, as representative examples. As may be observed, the volume deformation ( $k\%$ ) is larger, the higher the pressures and temperatures. Negative  $k\%$  values in compression and decompression steps are possibly due to changes from helicoidal to planar, and planar to helicoidal conformations<sup>5</sup> respectively. PEO time-dependent volume (see Figure 3; the retardation times depend on temperature, pressure, and instantaneous state,  $\Delta V/V_0$ , of the polymer)<sup>10,11</sup> extends over two decades of logarithmic times.

The bulk compression creep compliance  $B(t)$  may be computed from the data of Figure 2 as follows:

$$B(t) = \frac{k(t)}{P} \quad (12)$$

A plot of  $B(t)$  versus  $t$  is shown in Figure 4a and 4b as a function of pressure and temperature respectively. These can be reduced to a master curve by shifting them along the coordinate axis (Figures 5 and 6).

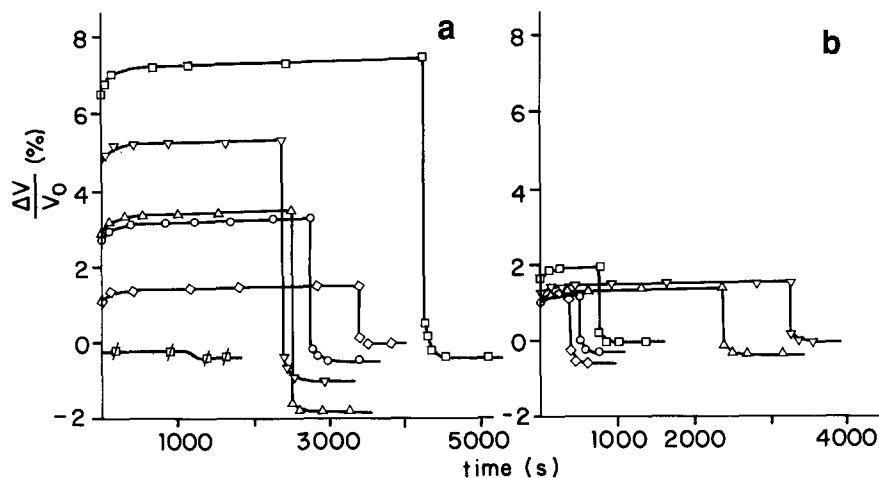


Figure 2 PEO volume deformation ( $k\%$ ) versus time ( $t$ ) as a function of (a) pressure at 403 K:  $\square$ , 5 MPa;  $\diamond$ , 30 MPa;  $\circ$ , 70 MPa;  $\Delta$ , 100 MPa;  $\nabla$ , 130 MPa;  $\square$ , 170 MPa; (b) temperature at 30 MPa:  $\diamond$ , 373 K;  $\circ$ , 383 K;  $\Delta$ , 393 K;  $\nabla$ , 403 K;  $\square$ , 412 K

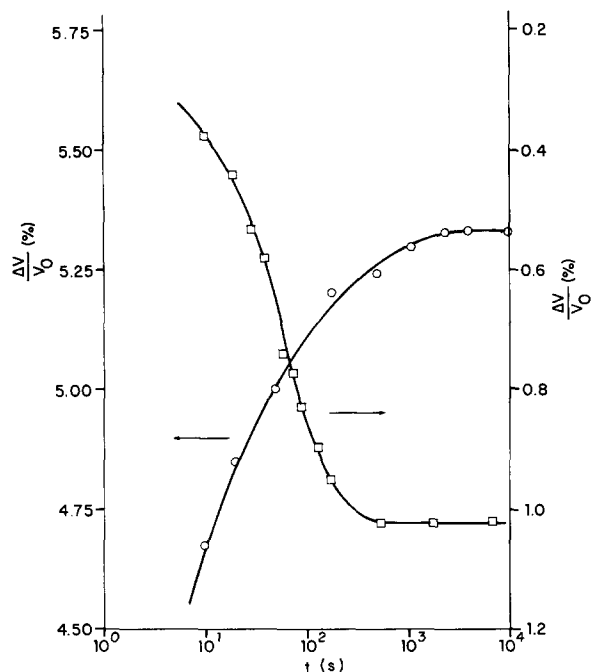


Figure 3 PEO volume deformation ( $k\%$ ) versus time ( $t$ ) at 403 K and 130 MPa;  $\circ$ , compression;  $\square$ , decompression

Pressure shift factors  $b_p$  and  $a_p$  (see Appendix B) were computed as follows<sup>10-12</sup>:

$$b_p = \frac{B(t, P_0)}{B(t, P)} \quad (13)$$

$$a_p = \frac{(\ln t)_{P_0}}{(\ln t)_P} \quad (14)$$

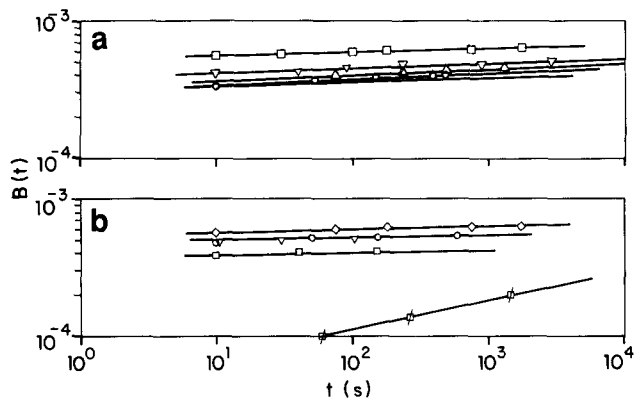


Figure 4 Bulk creep compliance  $B(t)$  versus time ( $t$ ) at: (a) 30 MPa and  $\circ$ , 383 K;  $\Delta$ , 393 K;  $\nabla$ , 403 K;  $\square$ , 412 K; (b) 412 K and  $\square$ , 5 MPa;  $\diamond$ , 30 MPa;  $\circ$ , 70 MPa;  $\nabla$ , 130 MPa;  $\square$ , 170 MPa

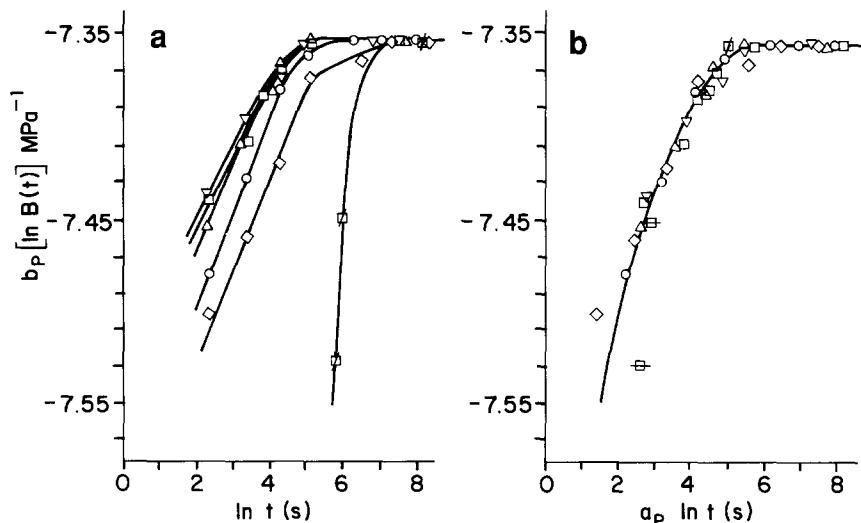


Figure 5 Bulk creep compliance  $B(t)$  as a function of pressure at  $T = 412$  K with reference pressure  $P_0 = 30$  MPa;  $\square$ , 5 MPa;  $\diamond$ , 30 MPa;  $\circ$ , 70 MPa;  $\Delta$ , 100 MPa;  $\nabla$ , 130 MPa;  $\square$ , 170 MPa; shifted parallel to (a) the ordinate axis ( $b_p$ ); (b) the abscissa axis ( $a_p$ )

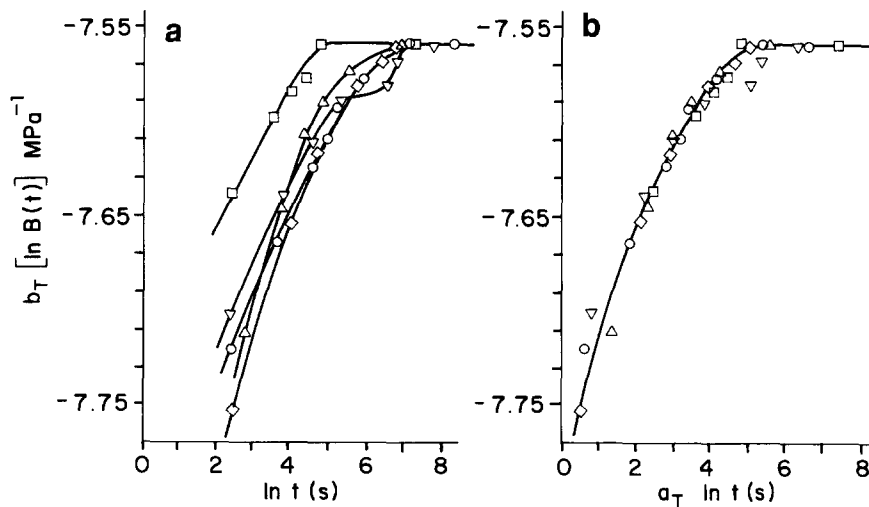


Figure 6 Bulk creep compliance  $B(t)$  as a function of temperature at  $P = 130$  MPa with reference temperature  $T_0 = 412$  K;  $\diamond$ , 373 K;  $\circ$ , 383 K;  $\Delta$ , 393 K;  $\nabla$ , 403 K;  $\square$ , 412 K; shifted parallel to (a) the ordinate axis ( $b_T$ ); (b) the abscissa axis ( $a_T$ )

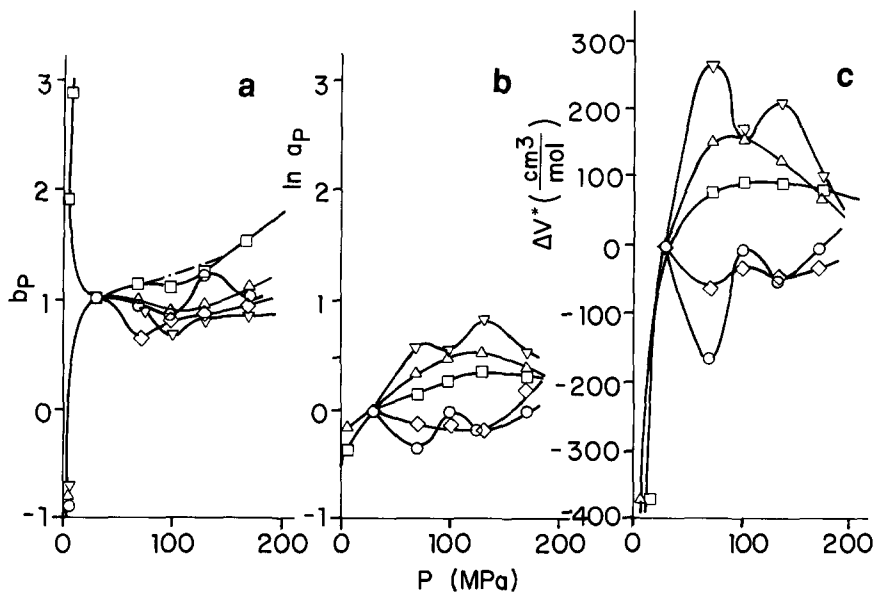


Figure 7 Pressure shift factors with reference pressure  $P_0 = 30$  MPa, at:  $\diamond$ , 373 K;  $\circ$ , 383 K;  $\Delta$ , 393 K;  $\nabla$ , 403 K;  $\square$ , 412 K. (a) Ordinate shift ( $b_p$ ); (b) abscissa shift ( $a_p$ ); (c) activation volume ( $\Delta V^*$ )

Figure 7 shows that  $b_p$  as well as  $a_p$  increase non-linearly as the compression stresses ( $P$ ) and temperature ( $T$ ) increase.

Temperature shift factors  $b_T$  and  $a_T$  (see Appendix B) were computed as follows<sup>10-12</sup>:

$$b_T = \frac{B(t, T)}{B(t, T_0)} \quad (15)$$

$$a_T = \frac{(\ln t)_T}{(\ln t)_{T_0}} \quad (16)$$

These factors increase as the temperature and pressure (except at 5 MPa) increase (Figure 8).

Bulk creep compliance  $B(t)$  behaviour (Figures 9a and 9b) is different below and above certain critical values of the process variables ( $T_c \approx 393$  K and  $P_c \approx 30$  MPa), a point presumed to be the transition from helicoidal to planar conformation<sup>5,12</sup>. Below this point, the behaviour is typical of helicoidal polymers: their large free volume (which gives their molecular segments greater mobility due to rotation about C-C bonds, bond angle deformation, change from *gauche* to *trans* conformations etc.) decreases the higher the applied stress ( $P$ ). Above this point PEO behaves as a zig-zag planar polymer, in which the compaction of the polymer chains freezes out the segmental mobility.

These molecular processes seem to account for the effectiveness of PEO in drag reduction applications<sup>5</sup>. In shear flow, a fluid interface between regions of high (near the wall) and low (centre of the pipe) deformation rates is produced. Polymer molecules migrate from the former into the latter region providing a low viscosity (polymer depleted) zone near the wall, possibly produced by the PEO changes from helicoidal to planar conformations under compression stresses.

The elastic energy storage recoverable after stress removal  $B_c$  is given by:

$$B_c = B_c^s - B_d^s \quad (17)$$

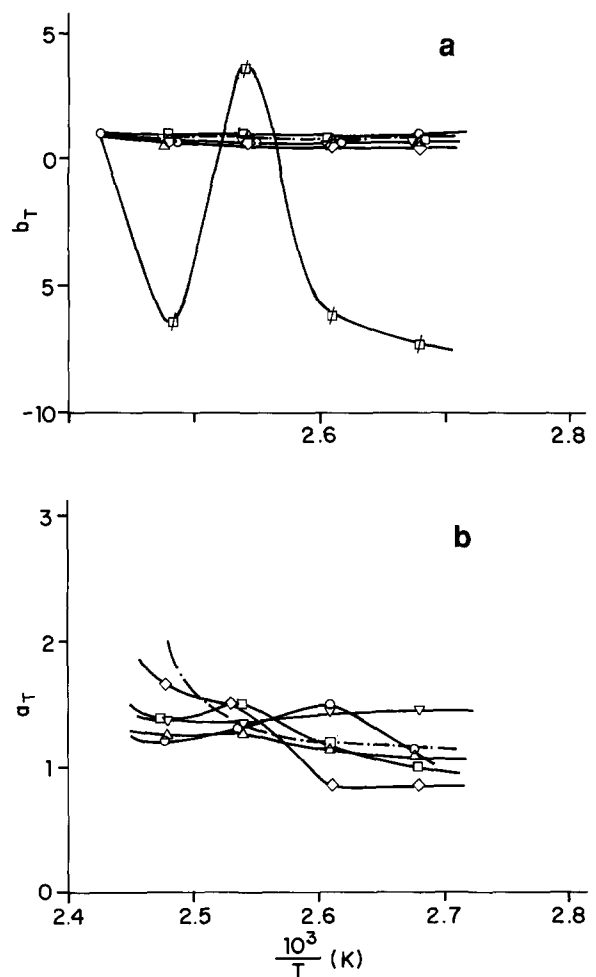
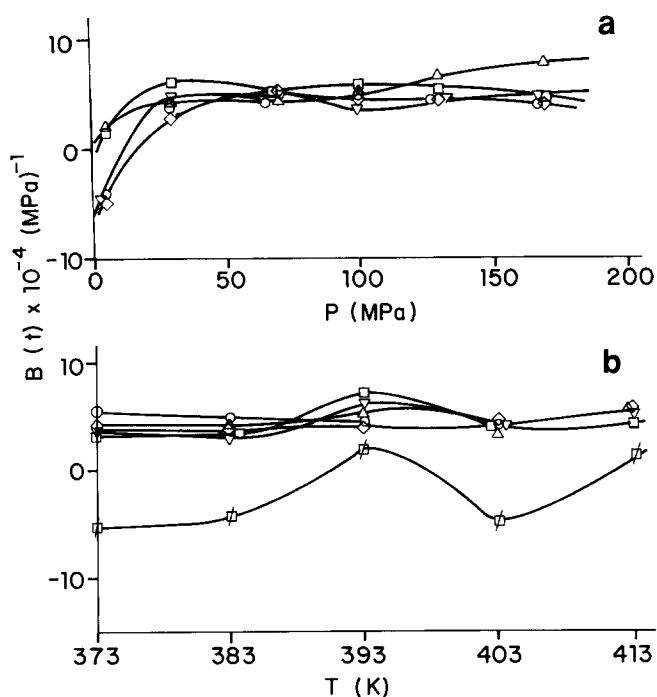
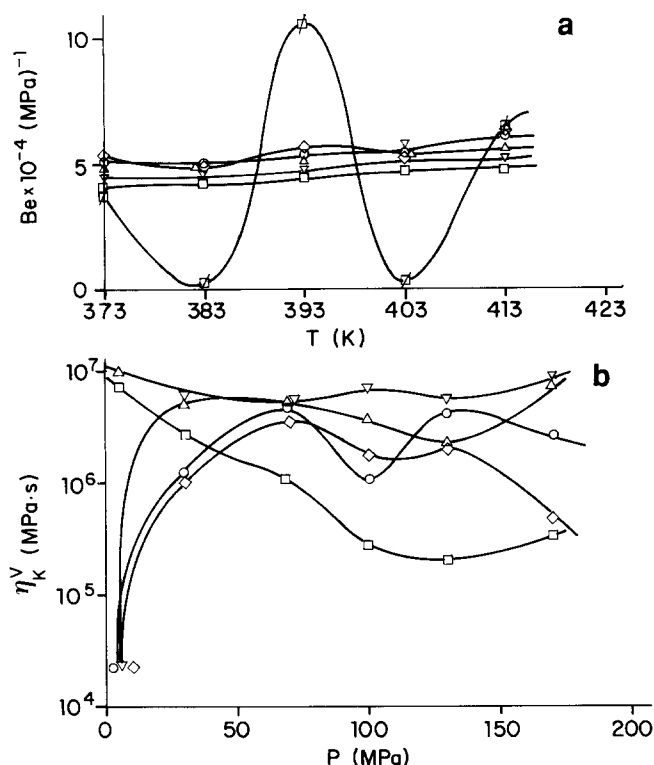


Figure 8 Temperature shift factors ( $b_T$  and  $a_T$ ) with reference temperature  $T_0 = 412$  K, at:  $\square$ , 5 MPa;  $\diamond$ , 30 MPa;  $\circ$ , 70 MPa;  $\Delta$ , 100 MPa;  $\nabla$ , 130 MPa;  $\square$ , 170 MPa. (a) Ordinate shift ( $b_T$ ); —, —, computed with equation (24); (b) abscissa shift ( $a_T$ ); —, —, computed with equation (26)



**Figure 9** Bulk creep compliance  $B(t)$  (a) as a function of pressure at:  $\diamond$ , 373 K;  $\circ$ , 383 K;  $\Delta$ , 393 K;  $\nabla$ , 403 K;  $\square$ , 412 K; (b) as a function of temperature at:  $\square$ , 5 MPa;  $\diamond$ , 30 MPa;  $\circ$ , 70 MPa;  $\Delta$ , 100 MPa;  $\nabla$ , 130 MPa;  $\square$ , 170 MPa



**Figure 10** (a) PEO steady state bulk creep compliance ( $B_e$ ) versus temperature at:  $\square$ , 5 MPa;  $\diamond$ , 30 MPa;  $\circ$ , 70 MPa;  $\Delta$ , 100 MPa;  $\nabla$ , 130 MPa;  $\square$ , 170 MPa. (b) PEO bulk viscosity ( $\eta_K$ ) as a function of stress ( $P$ ) at:  $\diamond$ , 373 K;  $\circ$ , 383 K;  $\Delta$ , 393 K;  $\nabla$ , 403 K;  $\square$ , 412 K

where  $B_e^c$  and  $B_e^d$  are the steady state creep compliance in the compression and decompression steps respectively. Values of  $B_e$  are plotted in Figure 10a (see also refs 2, 4 and Figures 7, 8, 9).  $B_e$  increases with increasing temperature and decreasing pressure.

The bulk (volume) viscosity ( $\eta_K$ ) is<sup>2,4</sup>:

$$\eta_K = \frac{-\Delta P}{\frac{\Delta V}{V_0} \frac{\Delta t}{l}} = \frac{\Delta t}{B_d^s} \quad (18)$$

Values of  $\eta_K$  are plotted in Figure 10b. Above 30 MPa,  $\eta_K$  remains almost constant as the pressure increases, whereas  $\eta_K$  decreases as the temperature increases (some scatter of data is observed, possibly due to the variation of the compression rates around  $0.5\text{--}2.0 \times 10^{-5} \text{ s}^{-1}$ ).

## CONCLUSIONS

Compression creep of molten polymers has been measured. PEO flexible chains show volume deformations ( $k\%$ ) which increase as the temperature increases (contrary to rigid chain polymers such as PS in which  $k\%$  decreases). The effects of temperature and pressure on bulk creep compliance  $B(t)$  are described by shift factors, the ordinate factors ( $b_T, b_P$ ) being governed by intramolecular interactions ( $\Delta H$ ), and the abscissa factors ( $a_T, a_P$ ) by activation energy ( $\Delta E$ ) and activation volume ( $\Delta V^*$ ). PEO bulk creep compliance  $B(t)$  behaviour is different below and above certain critical values ( $T_c, P_c$ ) of the process variables, corresponding to a change of chain conformation from helicoidal to planar. This provides a molecular explanation for the effectiveness of PEO in drag reduction applications. Bulk viscosity ( $\eta_K$ ) data follow the pattern of the molecular motions just described.

## REFERENCES

- 1 Aleman, J. V. *Rheol. Acta* 1988, **27**, 634
- 2 Aleman, J. V. *Angew. Makromol. Chem.* 1990, **181**, 53
- 3 Theocaris, P. S. *Kolloid Z u Z Polymere* 1972, **250**, 263
- 4 Aleman, J. V. *J. Appl. Polym. Sci.* in press
- 5 Aleman, J. V. *J. Non-Newtonian Fluid Mech.* 1987, **25**, 365
- 6 Lesbats, J. P., Legross, R. and Aleman, J. V. *J. Polym. Sci., Polym. Chem. Edn* 1982, **20**, 1971
- 7 Mark, H. F. and Bikales, N. (Eds) 'Encyclopedia of Polymer Science and Technology', Interscience Publishers, New York, 1967, Vol. 6, pp. 103-145
- 8 Bortel, E., Horodowicz, S. and Lamot, R. *Makromol. Chem.* 1979, **180**, 2491
- 9 Ming, L., Reind, G. G. and Zoller, P. *Polymer* 1988, **29**, 1784
- 10 Kovacs, A. J. *Trans. Soc. Rheol.* 1961, **5**, 285
- 11 Tribone, J. J. and O'Reilly, J. M. *J. Polym. Sci., Polym. Phys. Edn* 1989, **27**, 837
- 12 Ferry, J. D. 'Viscoelastic Properties of Polymers', Wiley, NY, 1980
- 13 Aleman, J. V. *Colloid Polym. Sci.* 1988, **266**, 975
- 14 Aleman, J. V. *Europ. Polym. J.* 1991, **27**, 221
- 15 Hartmann, B. and Balizer, E. *J. Appl. Polym. Sci.* 1986, **31**, 2377

## APPENDIX A

### Rigid and flexible polymers

Polymers may be classified<sup>14</sup> according to the mobility of their chain segments, resulting from:

1. Intramolecular interactions ( $\Delta H$ ) which include: (a) the potential energy hindering the internal rotation around a single bond; (b) repulsive forces and van der Waals attraction between non-bonded atoms or groups; (c) electrostatic interactions; and (d) hydrogen bonding.
2. Intermolecular interactions ( $T\Delta S$ ), which include (b), (c) and (d), as well as the efficient packing of the molecules as an integrated effect.

Accordingly, the melt chain rigidity may be considered to be<sup>6</sup> the Gibbs free energy of the system ( $-\Delta F$ ) composed of the intramolecular (enthalpy,  $\Delta H$ ) and intermolecular (entropy,  $T\Delta S$ ) interactions, which may be computed by graphical integration of specific heat ( $C_p$ ) versus temperature ( $T$ ) curves, according to the equations:

$$\Delta H = H_T - H_0 = \int_0^T C_p dT \quad (19)$$

$$\Delta S = S_T - S_0 = \int_0^T C_p \frac{dT}{T} \quad (20)$$

$$\Delta F = F_T - F_0 = \Delta H - T\Delta S \quad (21)$$

## APPENDIX B

### Pressure and temperature shift factors

Bulk creep compliance  $B(t)$  is the reciprocal of the bulk compression modulus of elasticity ( $L = P/(\Delta V/V_0)$ )<sup>14</sup>. When  $L$  is plotted versus the intramolecular interactions at 450 K ( $\Delta H$  in equation (19)); the decrease in  $C_p$  with increasing  $P$  is usually smaller than the experimental errors of the measurements<sup>15</sup>, a straight line results<sup>13,14</sup> which obeys the equation:

$$L = L_0 - \alpha \Delta H^{450K} \quad (22)$$

with  $L_0 \approx 4000$  MPa and  $\alpha \approx 2.5$  MPa ( $J g^{-1}$ )<sup>-1</sup>. Con-

sequently, the following equations are obtained:

$$b_p = \frac{L(P)}{L(P_0)} = \frac{L_0 - \alpha(\Delta H)_P}{L_0 - \alpha(\Delta H)_{P_0}} \quad (23)$$

$$b_T = \frac{L(T_0)}{L(T)} = \frac{L_0 - \alpha(\Delta H)_{T_0}}{L_0 - \alpha(\Delta H)_T} \quad (24)$$

Results according to these equations are plotted in Figures 7 and 8 (dashed lines).

$a_p$  has been described in the glassy state with the equation<sup>10,11</sup>:

$$a_p = \exp\left(\frac{\Delta V^*}{RT_0} P\right) \quad (25)$$

where  $R$  is the gas constant. A plot of  $\ln a_p$  versus  $P$  should provide straight lines (Figure 7b).  $\Delta V^*$  is the activation volume of value, except at 5 MPa, about  $-50$  to  $+200$  cm mol<sup>-1</sup> (with reference zero value that at 30 MPa, see Figure 7c). The same scatter of data has always been observed with flexible chain polymers<sup>4,5</sup>, because their large volume changes cause the non-linear response of the free volume to be more noticeable.

$a_T$  obeys the equation:

$$a_T = \exp\left(\frac{\Delta E}{R(T - T_0)}\right) \quad (26)$$

$\Delta E = 48$  kJ mol<sup>-1</sup> (ref. 5) is the PEO compression flow activation energy. Results are shown in Figure 8b (dashed line).